Cell

Exocytosis of Post-Golgi Vesicles Is Regulated by Components of the Endocytic Machinery

Jyoti K. Jaiswal,[1,3,*] Victor M. Rivera,[2] and Sanford M. Simon[1,*]
[1]The Rockefeller University, 1230 York Avenue, Box 304, New York, NY 10065, USA
[2]ARIAD Gene Therapeutics, Inc., 26 Landsdowne Street, Cambridge, MA 02139, USA
[3]Present address: Center for Genetic Medicine Research, Children's National Medical Center, Washington DC 20010, USA
*Correspondence: jaiswaj@rockefeller.edu (J.K.J.), simon@rockefeller.edu (S.M.S.)
DOI 10.1016/j.cell.2009.04.064

SUMMARY

Post-Golgi vesicles target and deliver most biosynthetic cargoes to the cell surface. However, the molecules and mechanisms involved in fusion of these vesicles are not well understood. We have employed a system to simultaneously monitor release of luminal and membrane biosynthetic cargoes from individual post-Golgi vesicles. Exocytosis of these vesicles is not calcium triggered. Release of luminal cargo can be accompanied by complete, partial, or no release of membrane cargo. Partial and no release of membrane cargo of a fusing vesicle are fates associated with kiss-and-run exocytosis, and we find that these are the predominant mode of post-Golgi vesicle exocytosis. Partial cargo release by post-Golgi vesicles occurs because of premature closure of the fusion pore and is modulated by the activity of clathrin, actin, and dynamin. Our results demonstrate that these components of the endocytic machinery modulate the nature and extent of biosynthetic cargo delivery by post-Golgi vesicles at the cell membrane.

INTRODUCTION

Eukaryotic cells use vesicles to carry newly synthesized lipids and proteins to and across the cell membrane. Secretory biosynthetic cargo is made in the endoplasmic reticulum (ER), traffics through the Golgi, and is packaged in vesicles that are transported to and fuse with the cell membrane, delivering their contents (Palade, 1975). Some of these vesicles (post-Golgi vesicles) fuse shortly after arriving at the cell surface (constitutive exocytosis), and other vesicles (synaptic and dense core vesicles) remain there until a transient rise in calcium triggers their fusion (regulated exocytosis). Regulated secretion involves control over formation and expansion of the fusion pore by regulators such as Ca^{2+} level (Ales et al., 1999; Elhamdani et al., 2006; Katz, 1971), synaptotagmin (Wang et al., 2001, 2006; Jaiswal et al., 2004), complexin (Archer et al., 2002; Barclay et al., 2005), Munc18 (Barclay et al., 2004, 2005), and PIP kinase Iγ (Gong et al., 2005).

It is known that a rapid influx of Ca^{2+} is not needed to trigger constitutive exocytosis (Miller and Moore, 1991; Edwardson and Daniels-Holgate, 1992; Lew and Simon, 1991). Thus, it is believed that release of cargo by post-Golgi vesicle exocytosis is not regulated by controlled formation and expansion of the fusion pore. However, while rapid Ca^{2+} influx does not trigger post-Golgi vesicle exocytosis, it is possible that efflux of Ca^{2+} from the lumen of the post-Golgi vesicle may control formation and expansion of the fusion pore during post-Golgi vesicle fusion. This has been observed in endosomes (Mayorga et al., 1994; Holroyd et al., 1999), yeast vacuoles (Peters and Mayer, 1998), and ER-to-Golgi and intra-Golgi carriers (Chen et al., 2002; Porat and Elazar, 2000). Moreover, mechanisms other than calcium increase, such as spontaneous reversal of fusion (Stevens and Williams, 2000) and the action of endocytic machinery (Holroyd et al., 2002; Newton et al., 2006; Graham et al., 2002), could regulate fusion pore of exocytic post-Golgi vesicles. Thus there is a need to investigate whether Ca^{2+}-dependent or independent mechanisms control formation and expansion of the post-Golgi vesicle fusion pore.

Two features that have enabled studying the regulation of cargo release by formation and expansion of the fusion pore during regulated exocytosis are (1) the ability to synchronize fusion by Ca^{2+} increase and (2) the use of fluorescently tagged luminal and membrane cargoes. As no triggering mechanism is known for post-Golgi vesicle exocytosis, in mammalian cells this synchrony has been achieved by altering growth temperature to block biosynthetic cargo traffic and then reverting to normal temperature to release the block. However, temperature affects not only fusion pore formation and expansion (Zhang and Jackson, 2008), but also distribution of lipids and dynamics of transport throughout the secretory pathway (Patterson et al., 2008). While constitutive secretion of biosynthetic membrane cargo has been monitored (Schmoranzer et al., 2000; Kreitzer et al., 2003), secretion of luminal cargo from individual post-Golgi vesicle has not been monitored. To study formation and expansion of fusion pores during post-Golgi cargo secretion, other approaches to synchronize, label and monitor exocytosis of post-Golgi vesicles are needed.

We had previously developed an approach to synchronize secretion of constitutive biosynthetic cargo by using a cell-permeable pharmacological regulator, to avoid shifting temperature (Rivera et al., 2000). This approach allows us to selectively control

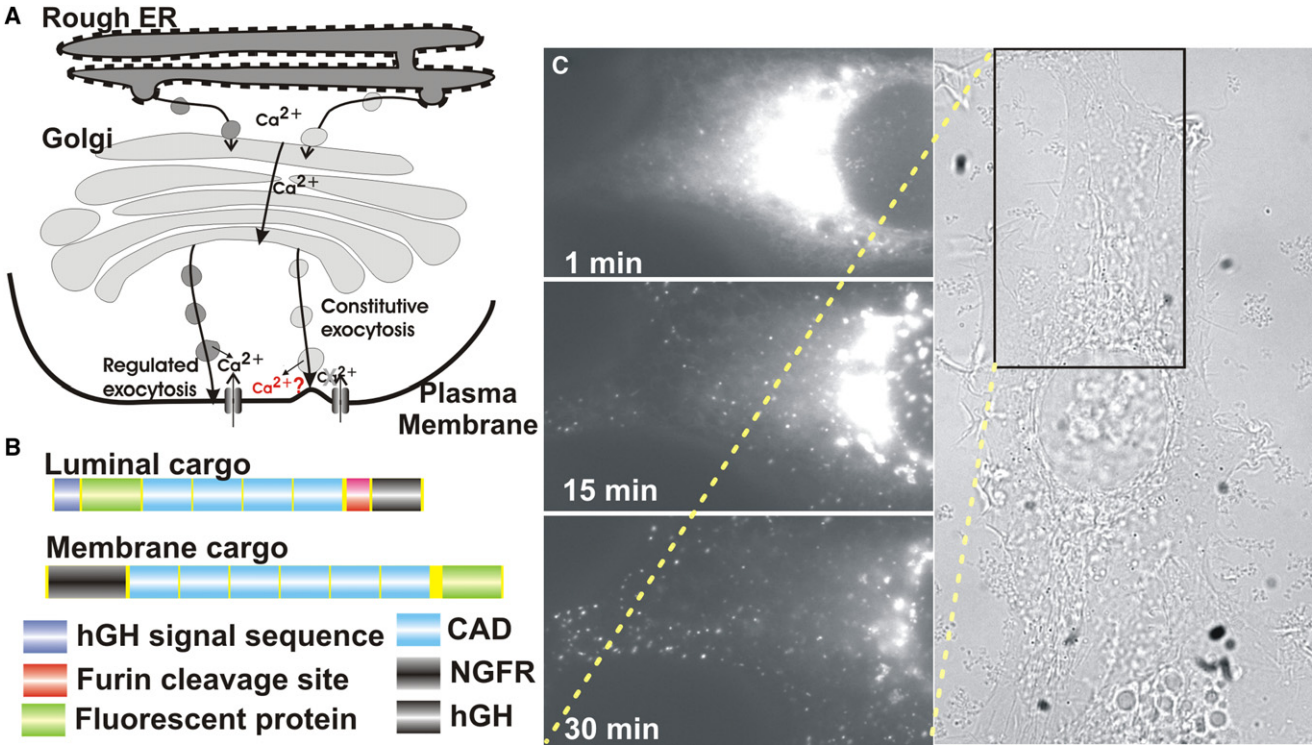

Figure 1. Regulation of Biosynthetic Cargo Trafficking

(A) Schematic showing two pathways for cell-surface delivery of biosynthetic cargo. In each pathway, places where cargo trafficking can be regulated by Ca^{2+} are marked. During regulated exocytosis, calcium increase due to influx from across the plasma membrane channels and efflux from the vesicle trigger exocytosis. In constitutive exocytosis of post-Golgi vesicles, entry of calcium through plasma membrane channels is not required for exocytosis, but it is not known whether the calcium released from docked post-Golgi vesicle triggers its exocytosis.

(B) Schematic showing different domains of the luminal and membrane cargoes used in this study.

(C) Epi-fluorescence (left) and phase contrast images (right) of a cell with the luminal cargo (GFP-CAD) at various time points after its release from the ER by the addition of AP21988.

trafficking of only the desired biosynthetic cargo (membrane or luminal). It is thus well suited for studying formation and expansion of fusion pores during post-Golgi cargo secretion. Here, we have used this approach together with total internal reflection fluorescence microscopy (TIRFM) to simultaneously image secretion of luminal and membrane cargo by individual post-Golgi vesicles in live cells. We found that post-Golgi vesicles can undergo partial (kiss-and-run) exocytosis, resulting in incomplete release of luminal cargo and partial or no release of membrane proteins. Ca^{2+} had no detectable effect on triggering post-Golgi vesicle fusion, nor did it affect the nature of post-Golgi vesicle exocytosis. Instead, clathrin, dynamin and actin—known regulators of endocytosis—control the nature and extent of post-Golgi vesicle exocytosis. Our results identify kiss-and-run exocytosis as a significant regulator of the extent of biosynthetic cargo secretion by post-Golgi vesicles. It also provides evidence that this control is achieved via the activity of the endocytic machinery.

RESULTS

Synchronization of Biosynthetic Cargo Secretion

To synchronize the delivery of biosynthetic cargo to the surface, we tagged the cargo of interest with F36M—a mutant version of protein FKBP12. F36M is termed as conditional aggregation domain (CAD) because its homodimerization is reversible by a small cell-permeant molecule AP21988 (Rivera et al., 2000; Rollins et al., 2000). After synthesis in the ER, proteins with multiple CADs self-aggregate and are retained there until ligand addition causes the cargo to disaggregate and traffic through the secretory pathway (Figure 1A) (Rivera et al., 2000). As a marker for luminal cargo, we expressed human growth hormone signal sequence (hGHss) fused to GFP, four CADs, and hGH. Our membrane marker was nerve growth factor receptor (NGFR), which we have previously used to mark the post-Golgi vesicle membrane (Kreitzer et al., 2003), expressed with a fluorescent protein and CADs (Figure 1B).

Within a few minutes of adding the CAD-disaggregating molecule AP21988 to the culture media, the fluorescence of the luminal cargo moved from the reticular distribution of the ER to a perinuclear distribution of the Golgi and then moved peripherally in small vesicles (Rivera et al., 2000) (Figure 1C; Movie S1 available online). Within 15 min of ligand addition, we detected individual fluorescent vesicles at the cell membrane by TIRFM (data not shown). To determine whether the fluorescent marker was in post-Golgi vesicles, we simultaneously expressed either the LDL receptor or VSVGts, as fusions to YFP (Schmoranzer

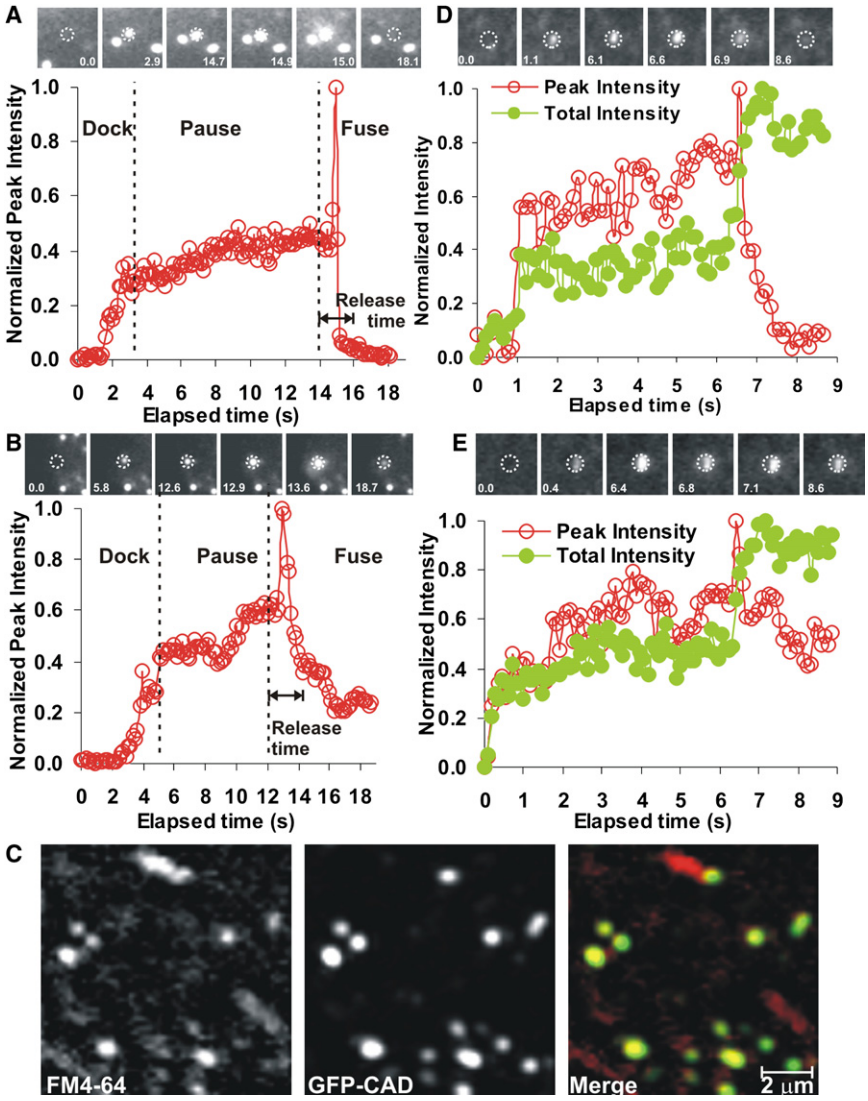

Figure 2. Imaging Individual Post-Golgi Vesicle Exocytosis

Exocytic vesicles are monitored using luminal marker GFP-CAD (A–C) and membrane marker NGFR-GFP (D and E). Complete release (A and D) and partial (kiss-and-run) release (B and E) of the cargoes are shown. The dotted circle marks pixels whose intensity was unchanged as the vesicle docked. The plots show fluorescence within the dotted circle (open symbols) and of the entire field (filled symbols). Intensity is normalized after background was subtracted prior to the appearance of the vesicle. A vesicle was considered to be tethered/docked at the point after appearing in the evanescent field when its fluorescence was relatively stable. Priming marks the period between docking and initiation of fusion, which is indicated by a rapid increase in vesicle fluorescence followed by the cargo release. As total fluorescence of the membrane cargo in (D) and (E) remain unchanged after release of the cargo from the vesicles, it indicates that the proteins from the vesicle membrane are delivered to the cell membrane and not lost in the cytosol (as would occur if the vesicle had lysed). A cell expressing GFP-CAD (green) that was treated for 20 min with AP21988, followed by 10 min in FM4-64 (red) is shown (C). The image is of a part of this cell showing many vesicles labeled with both these markers.

et al., 2000). In cells at 20°C, LDLR is retained in the TGN, whereas at 40°C, VSVGts is retained in the ER. Both proteins traffic via post-Golgi vesicles upon shifting of cells to 37°C (Schmoranzer et al., 2000). The CFP-tagged luminal or membrane marker colocalized with the vesicles carrying YFP-tagged LDLR or VSVGts (correlation coefficient 0.79 and 0.80, respectively; Figures S1A, S1B, S1E, and S1G). This indicated that the cell membrane-proximal vesicles carrying the CAD-containing fluorescent proteins were bona fide post-Golgi vesicles.

Post-Golgi Vesicles Undergo Kiss-and-Run Exocytosis

To monitor secretion of cargo from these post-Golgi vesicles, we imaged cells expressing hGHss-GFP-CAD-hGH by TIRFM. During transit through the ER and Golgi, hGHss and hGH are cleaved from this protein. Thus, the fluorescent vesicle luminal marker is GFP fused to the CADs (GFP-CAD) (Rivera et al., 2000) (Figure 1B). The fluorescence of these vesicles increased as they entered the evanescent field, and then dropped rapidly to background level as it spread laterally, indicating cargo exocytosis (Figure 2A). We also observed exocytic events where vesicle fluorescence decreased, but remained above the background (Figure 2B). This observation is consistent with the vesicle transiently opening its fusion pore to the outside, releasing only a part of its cargo. The fact that most of these vesicles do not move after fusion notwithstanding, the term "kiss-and-run fusion" is used to describe such partial fusion fates (Harata et al., 2006). We will thus refer to these fusion fates as kiss-and-run fusion. To test whether these partially fusing vesicles open a transient fusion pore, we used FM4-64 dye, which can access the vesicle membrane only when it contacts the extracellular media and has been used to test kiss-and-run fusion of synaptic and other vesicles (Harata et al., 2006). Indeed, FM4-64 labeled many GFP-containing post-Golgi vesicles (Figure 2C). Similarly, vesicles were labeled with the fluid phase marker Alexa fluor 546-hydrazine (data not shown).

The ability of extracellular markers to enter the lumen of the vesicle indicates that partial release of the luminal marker is due to a transient opening to the outside. However, it does not rule out the possibility that this may involve photodamage to the cell and vesicle membrane, causing mixing of luminal and extracellular contents. To resolve between fusion, leakage, and lysis, we monitored the fate of vesicle membrane proteins during exocytosis. Only upon exocytosis of a vesicle will its membrane protein be delivered to the cell surface where it diffuses in two

dimensions; thus, any decrease in vesicle fluorescence will cause a concomitant increase in cell membrane fluorescence, resulting in no change in integrated fluorescence. In case of leakage, the membrane marker would remain with the vesicle and not diffuse in the cell membrane, whereas in case of lysis, it will diffuse in the cytoplasm in three dimensions (Jaiswal and Simon, 2007; Jaiswal et al., 2007; Schmoranzer et al., 2000). After ligand addition, CFP-tagged CAD-NGFR trafficked to the post-Golgi vesicles together with YFP tagged CAD (Figures S1C and S1D). Based on the fluorescence of the vesicle membrane marker, we observed two types of exocytic behaviors. In some cases, the fluorescence of the vesicular membrane protein reduced to the predocking background (Figure 2D, red symbol), indicating complete release. In other cases, the fluorescence of the vesicular membrane protein decreased, but remained above the predocking background (Figure 2E, red symbol), indicating partial release. In each of the observed fates of the vesicle (Figures 2D and 2E), the integrated (sum of vesicular and cell membrane) fluorescence of the fusing vesicle's membrane protein remained high (green symbols) even when there was a decrease in the luminal fluorescence (red symbols). This confirms that these events involve merger of the vesicle and cell membrane and thus indicate exocytosis, not leakage or lysis.

To quantify the number of post-Golgi vesicles undergoing partial or complete fusion, we monitored the release of the luminal cargo or membrane cargo after the addition of CAD-disaggregating ligand. Based on luminal contents (GFP-CAD), we observed 32.7 ± 8.0 fusions/cell in a minute, of which 73% (23.8 ± 7.1) were kiss-and-run fusions and the rest (8.9 ± 2.9) were complete fusions (Figure 3A, gray bars). In contrast, using membrane cargo (NGFR-GFP), we observed only 12.2 ± 2.2 fusions/cell in a minute, of which 17% (2.1 ± 0.8) were kiss-and-run fusions and the rest 10.1 ± 2 were complete fusions (Figure 3A, black bars). While the difference in the number of complete fusions reported by luminal and membrane markers is not statistically significant ($p = 0.4$), there is an 11-fold difference in the number of vesicles that partially released their content ($p = 10^{-6}$). These results are consistent with a population of vesicles that undergo kiss-and-run fusion, resulting in partial release of their luminal cargo but no release of the membrane cargo. To test this prediction, we coexpressed the membrane and luminal markers as CFP- and YFP-tagged proteins. Both of these cargoes were sequestered in the ER, and after addition of AP21988 they were packaged in the same post-Golgi vesicles (Figures S1C, S1D, and S2A–S2C).

Quantification of the vesicle- and cell membrane-associated fluorescence indicates vesicles that fully released their YFP-tagged luminal cargo (Figure 3B, red line) also fully released their CFP-tagged membrane marker cargo (Figure 3B, open blue circles), and the released membrane cargo is delivered to the cell membrane: the integrated fluorescence of the vesicle and cell membrane remained relatively constant after exocytosis (Figure 3B, green line, filled symbols). Thus, vesicle luminal and membrane cargoes behaved similarly when coexpressed or expressed independently—their fluorescence returned to prefusion level (Figures 2A and 2D). Vesicles partially releasing their luminal content delivered either little or no membrane protein (Figures 3C–3E, S2B, and S2C). The fusion events where luminal cargo was partially released and membrane cargo was not released (state 3 in Figure 3E) account for the reduced number of partial fusions when only the vesicle membrane protein was used as exocytic marker (Figure 3A). To examine whether restricted fusion pore also slows release of luminal content during kiss-and-run fusion, we compared the time between start and end of luminal cargo release by individual exocytic vesicles from five cells. Cargo released faster during complete fusions (1.11 ± 0.30 s) compared to kiss-and-run fusions (1.49 ± 0.36 s) ($p = 0.01$; Figure 3F).

It has been previously reported that dense core vesicles (DCVs) can partially release their luminal contents together with release of some membrane proteins, but not others (Tsuboi et al., 2004). This was interpreted as a restriction on the ability of specific cargo to be released. Thus, incomplete release of membrane proteins could reflect a limitation of the particular reporter protein used and not the nature of the fusion. However, there are two observations, which indicate that this conclusion is not applicable to our membrane reporter, NGFR-GFP. First, our observation that ~17% (2/12; Figure 3A) of post-Golgi vesicles containing the membrane protein NGFR-GFP undergo kiss-and-run fusion is consistent with the value we have observed with other biosynthetic membrane proteins. For example, we previously reported that 14% of vesicles labeled with the membrane protein LDLR-GFP undergo kiss-and-run fusion (Schmoranzer and Simon, 2003). Second, we find that a vesicle that undergoes kiss-and-run fusion with no release of membrane cargo can subsequently fuse and release its membrane cargo partially or completely (Figure 3D). Thus, the very same membrane cargo can be observed to not release, partially release, and then fully release from the very same vesicle. The fluorescence intensity changes observed in Figure 3D potentially can be accounted by successive fusion of multiple colocalized vesicles with different exocytic fates (Figure S2D). To test whether the fluorescence originated from a single or multiple vesicles, we curve fitted the observed fluorescence intensity profiles (Figure S2E). The fluorescence profile best fits a single source of <100 nm, confirming that the fluorescence signals we observed originated from a single post-Golgi vesicle undergoing multiple fusions (Figures S2D and S2E). Together, these results suggest that the incomplete release we observe is not a limitation of our reporter. Instead, it is consistent with a restriction in the dilation of the fusion pore similar to what is proposed for kiss-and-run fusion of regulated exocytic vesicles (Harata et al., 2006).

Ca^{2+} Does Not Trigger or Regulate the Nature of Post-Golgi Vesicle Exocytosis

Unlike regulated exocytic vesicles, exocytosis of post-Golgi vesicles is unaffected when extracellular Ca^{2+} is chelated with EGTA (Lew and Simon, 1991). This indicates that Ca^{2+} influx is not required for post-Golgi vesicle exocytosis, but does not rule out that transient localized Ca^{2+} microdomains formed by the efflux from the docked post-Golgi vesicle may trigger its exocytosis. Such a mode of Ca^{2+} triggering has been identified for other membrane fusion reactions (Peters and Mayer, 1998). To test this possibility, we used two reagents—ionomycin to rapidly discharge vesicular Ca^{2+} (Williams et al., 1985), and

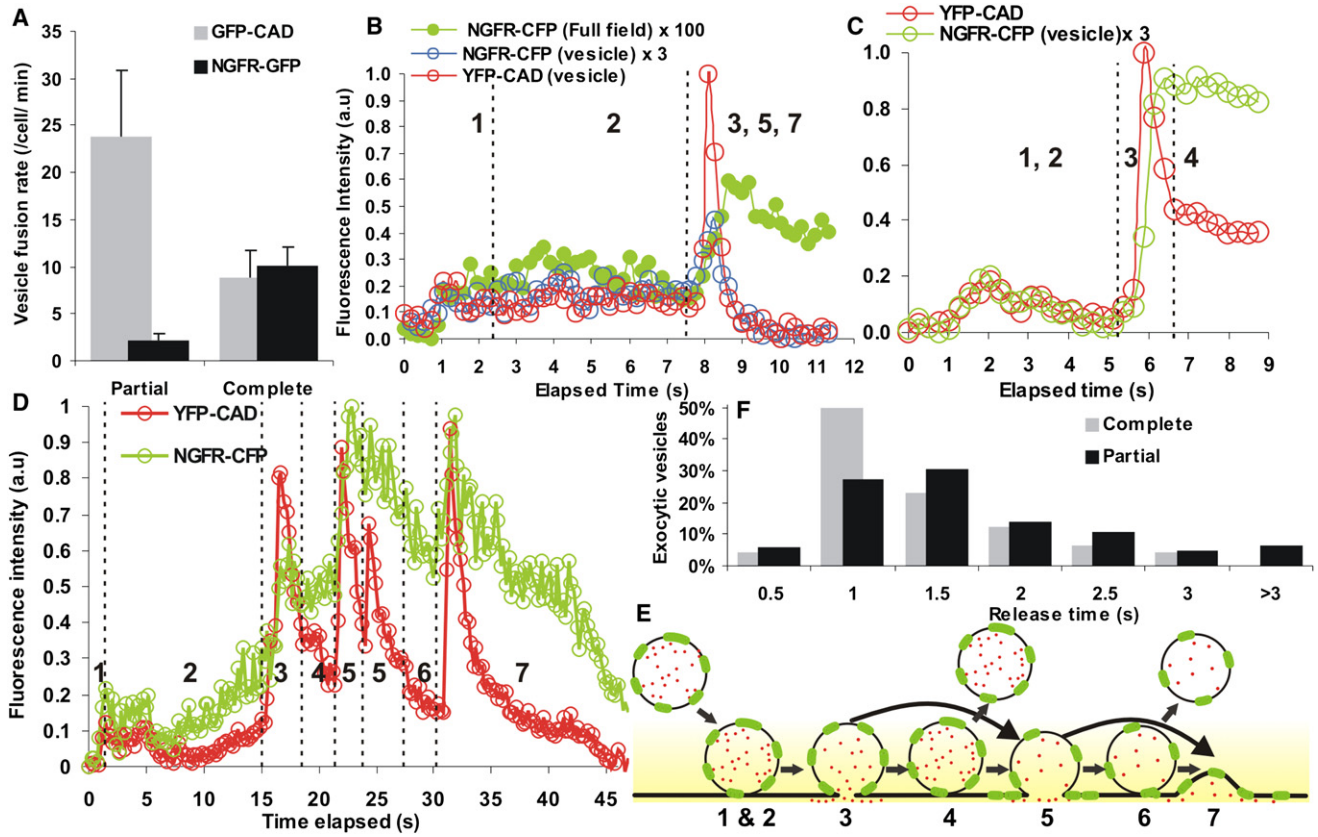

Figure 3. Post-Golgi Vesicles Can Exocytose without Releasing Membrane Cargo

(A) Vesicles undergoing partial (kiss-and-run) or complete exocytosis were measured for 1 min in cells expressing only luminal (n = 378 vesicles from nine cells) or only membrane (n = 135 vesicles from six cells) markers. The error bars represent the standard deviation.

(B) A vesicle labeled with both luminal (YFP-CAD) and membrane (NGFR-CFP) marker (Figure S2A) that undergoes complete fusion. An open symbol shows vesicle-associated fluorescence, and a filled symbol shows fluorescence of the entire field of view.

(C) A dual-labeled vesicle that exocytoses to partially release the luminal cargo (red symbol), but does not deliver any membrane cargo to the cell surface (green symbol). Images of this vesicle during fusion are shown in Figure S2B.

(D) Total fluorescence of luminal and membrane cargo for a vesicle that undergoes multiple partial fusions prior to complete fusion. This vesicle is shown in Figure S2C, and a schematic for the various fusion stages are marked by numbers as described in (E).

(E) Schematic showing states of the vesicle imaged in (D). 1 & 2: Docking and priming. 3: First fusion with the cell membrane resulting in partial release of luminal marker (rapid increase and decrease in YFP fluorescence) and no release of the membrane marker (increase and no subsequent decrease in the vesicle associated CFP fluorescence). 4: A period where none of the two markers were released from the vesicle. 5: Fusion where the luminal and membrane markers are released partially albeit to different extents. 6: A period when both the markers are retained by the vesicle. 7: Complete release of luminal and membrane cargoes resulting in return of their vesicle associated fluorescence to pre-docking background. Membrane cargo is marked in green, and luminal cargo in red; the shaded yellow region depicts the evanescent field.

(F) Release time for hGHss-GFP was quantified for vesicles that underwent partial or complete fusion in five cells (n = 169 vesicles). Release time denotes the period during which vesicle fluorescence increased and reached a postfusion plateau (see Figure 2).

BAPTA-AM to rapidly chelate cytosolic Ca^{2+} and prevent the formation of Ca^{2+} microdomains (Peters and Mayer, 1998). Increase of Ca^{2+} by ionomycin triggered lysosomal exocytosis in HT1080 cells, as we have previously observed for other cells (Jaiswal et al., 2002). BAPTA-AM prevents Ca^{2+} microdomain formation, which triggers yeast vacuole fusion (Peters and Mayer, 1998). Using the Ca^{2+}-sensitive ratiometric dye pair fura-red and fluo-3, we found that both these agents stably altered the cytosolic Ca^{2+} within 10 s (Figure 4A). Calcium is required for trafficking of biosynthetic cargo from ER to Golgi (Beckers and Balch, 1989), and this treatment reduced the number of fluorescently labeled post-Golgi vesicles that newly appeared in the TIR field (Movie S2). Thus, assay of total cargo released from cells with altered cytosolic calcium cannot distinguish between effects of Ca^{2+} on vesicle exocytosis and effects on transport through the biosynthetic pathway.

To resolve whether calcium affected steps after transport, we took advantage of the observation that most post-Golgi vesicles pause prior to fusion, as if briefly tethered to the cell membrane (step 2 in Figure 3E; Figure 4B, n = 107) (Schmoranzer et al., 2000). Exocytosis of these cargo-carrying post-Golgi vesicles is independent of effects at the step of cargo packaging. Thus, we monitored the membrane-tethered post-Golgi vesicles to test for effects of calcium release from their lumen on exocytosis.

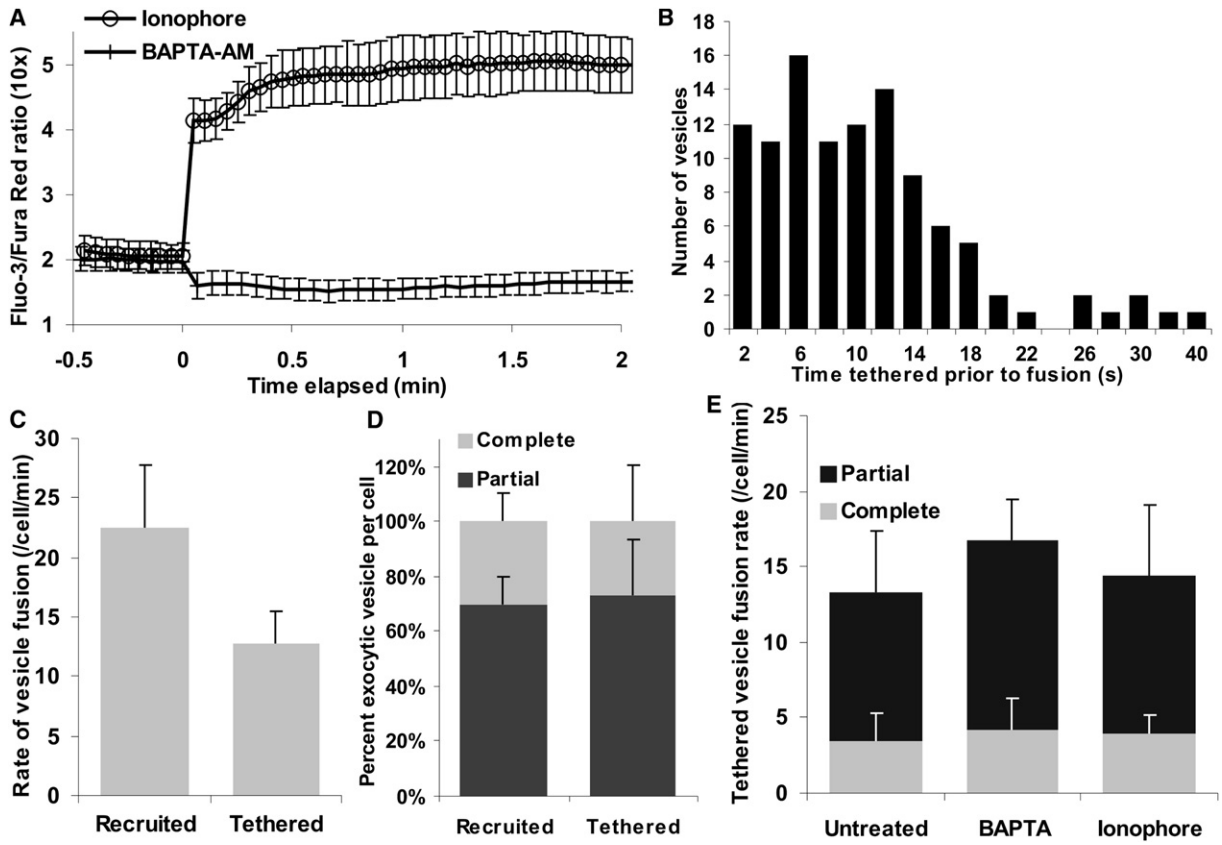

Figure 4. Effect of Calcium on Trafficking and Exocytosis of Post-Golgi Cargo

(A) Six HT1080 cells labeled with Fura-red and Fluo-3 and were imaged with epifluorescence excitation starting 30 s prior to the addition of calcium-altering agents, and their averaged fluorecence is plotted.

(B) Cells expressing luminal cargo GFP-CAD were imaged by TIR-FM, and the time for which the exocytic vesicles remained tethered at the cell surface prior to fusion was measured for 107 vesicles.

(C) Rate of exocytosis of 450 GFP-CAD-labeled vesicles from ten cells was quantified; those present in the TIR field at the start of imaging were termed as tethered/docked, and the rest were classified as recruited.

(D) Exocytic fate of the tethered and newly recruited vesicles.

(E) Tethered post-Golgi vesicles that underwent exocytosis were quantified in nine cells each that were treated for 20–40 min with AP21988 only (untreated) or with AP21988 followed by 100 μM BAPTA-AM (for 5 min) or 10 μM ionomycin.

The error bars represent the standard deviation.

In cells where calcium has not been altered, over one-third of all vesicles that exocytosed during a 2 min imaging period were tethered at the cell surface at the start of imaging (Figure 4C). Vesicles that were tethered or freshly recruited were equally likely to partially (or completely) release their contents (Figure 4D). We next quantified the effect of transient treatment of ionomycin or BAPTA-AM on exocytosis of tethered vesicles (Figure 4E). Neither chelating the cytosolic Ca^{2+} (with BAPTA-AM) nor increasing it (with ionomycin) affected the rate of exocytosis of post-Golgi vesicles (Figure 4E, $p > 0.4$ for both treatments). To test whether the acidic lumen of secretory vesicles was hindering the ionomycin-induced release of calcium, we treated cells with ionomycin in the presence of 25 mM NH_4Cl or 100 μM of the Na^+/H^+ exchanger monensin. Neither agent alone or together with ionomycin had any affect on the rates of post-Golgi vesicle fusion (data not shown). These results indicate that post-Golgi vesicle exocytosis is insensitive to calcium influx and insensitive to any local Ca^{2+} efflux from the secreting vesicle. To test whether Ca^{2+} affects the nature of post-Golgi vesicle fusion, we monitored post-Golgi vesicle exocytosis in BAPTA and ionomycin-treated cells. We detected no changes in the rate of partial or complete release of cargo by either treatment (Figure 4E; p values between 0.2 and 0.8). This ruled out a role of Ca^{2+} or Ca^{2+}-dependent exocytic machinery in regulating the choice between kiss-and-run and complete fusion of post-Golgi vesicles.

Endocytic Machinery Affects the Nature of Post-Golgi Vesicle Exocytosis

We examined whether clathrin, actin, and dynamin, proteins that control membrane curvature, bending, and fission during endocytosis, affect kiss-and-run fusion of post-Golgi vesicles. We immunostained the cells treated with AP21988 (to allow GFP-CAD to traffic into the post-Golgi vesicles) for endogenous

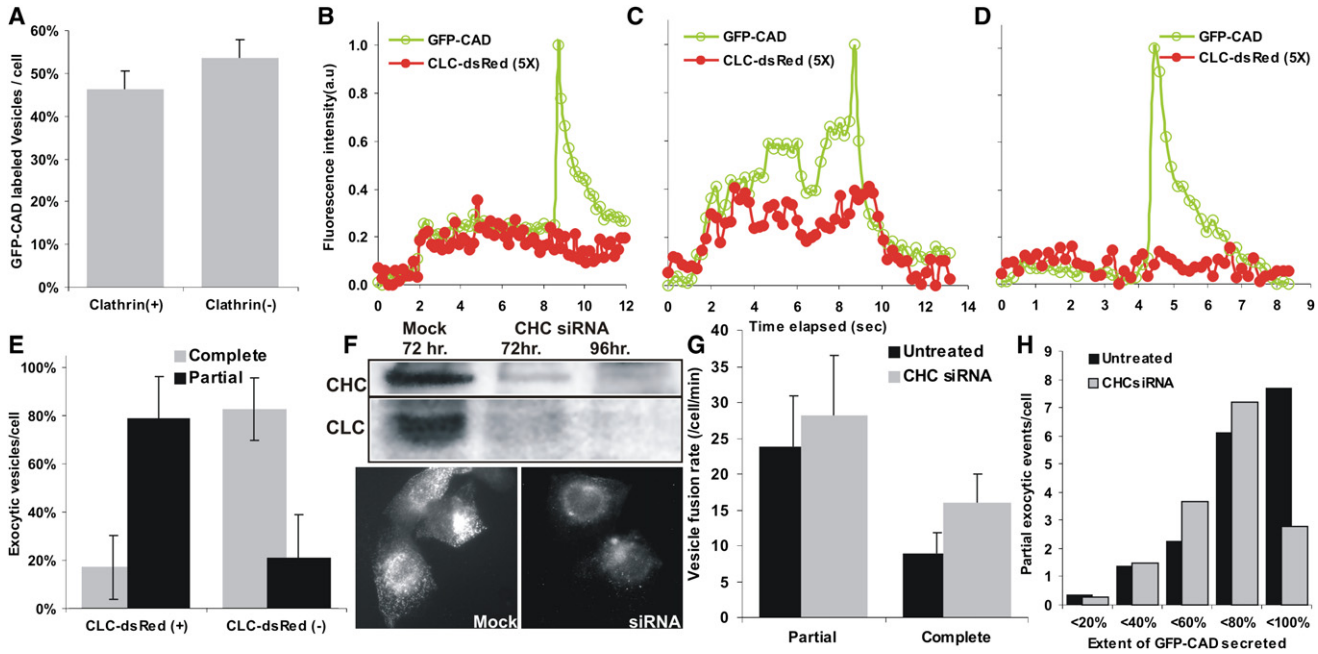

Figure 5. Role of Clathrin on the Nature of Post-Golgi Vesicle Exocytosis

(A) Cells treated with AP21988 to label post-Golgi vesicles with GFP-CAD were fixed and immunostained for CLC, and 245 GFP-labeled vesicles were scored for the presence of clathrin.

(B–D) Change in dsRed-CLC signal associated with vesicles that undergo kiss-and-run (B and C) or complete (D) fusion.

(E) A plot showing secretory fates of 118 GFP-CAD-labeled exocytic vesicles from four cells expressing dsRed-CLC. Vesicles were scored for the presence (+) or absence (−) of dsRed-CLC.

(F) Efficacy of siRNA-mediated knockdown of clathrin examined by immunoblotting and immunofluorescence.

(G) Effect of clathrin knockdown on the exocytic fate of 543 and 565 GFP-CAD vesicles, respectively, from nine cells, each of which were untreated or treated with CHC siRNA.

(H) Extent of GFP-CAD secreted by vesicles undergoing kiss-and-run fusion in untreated and CHC-siRNA-treated cells.

The error bars represent the standard deviation.

clathrin light chain. Half of all the vesicles analyzed (n = 245) from four cells contained a detectable endogenous clathrin signal (Figures 5A and S3A). To determine whether this colocalization was functionally associated with the nature of vesicle fusion, we simultaneously imaged luminal post-Golgi cargo (GFP-CAD) and dsRed-clathrin light chain (CLC) in live cells (Movie S3). Expression of dsRed-CLC had no effect on the nature of the secretion of luminal cargo GFP-CAD (data not shown). A majority (71 out of 118) of the exocytic post-Golgi vesicles containing GFP-CAD were also labeled with dsRed-CLC (vesicle marked with circle in Movie S3; Figures 5B and 5C), and 79% of such clathrin labeled vesicles underwent kiss-and-run fusion (Figure 5E). Clathrin was present on the vesicles prior to docking. In some of the vesicles, CLC-dsRed did not dissociate even after fusion (Figure 5B); in others, it dissociated after fusion (Figure 5C). Of the vesicles with no detectable dsRed-CLC (vesicle marked with square in Movie S3; Figure 5D), 83% completely released their contents (Figure 5E). To test whether clathrin affects post-Golgi vesicle exocytosis, we reduced the expression of clathrin heavy chain (CHC) and CLC by over 80% (Figure 5F) using a previously described small interfering RNA (siRNA) (Hinrichsen et al., 2003). With this siRNA, the cells had very little punctate CLC staining and some residual perinuclear staining (Figure 5F, lower panel), consistent with previous reports (Hinrichsen et al., 2003). The cells showed a nearly 2-fold increase (16 ± 4 versus 8.9 ± 2.9; p = 0.001) in complete fusions and increase in total rate of fusion from 32.7 ± 8 to 44.2 ± 10.1(p = 0.02) (Figure 5G). However, there was no change in the rate of kiss-and-run fusion (p = 0.3). As there is a broad distribution (from <20% to <100%) of the amount of luminal cargo released by vesicles undergoing kiss-and-run fusion, we tested the effect of CHC knockdown on this distribution. In CHC siRNA-treated cells, there are more vesicles in all bins where cargo released is <80% (Figure 5H). However, the number of vesicles that release between 80% to <100% of their cargo decreased ~3-fold. This shows that knockdown of CHC affects vesicles undergoing partial fusion such that some vesicles with no detectable release of their content (nonexocytic vesicles) in untreated cells now release between 20% and 80% of their content, causing an increase in these bins. But vesicles that release between 80% and <100% of their content now release all of their content (complete release), causing a decrease in <100% bin. Thus, through its effect on vesicles that normally do not fuse and fuse partially, CHC knockdown caused an increase in number of complete fusions and total number of fusion events.

We next examined the association of dynamin with post-Golgi vesicles. Thirty minutes after the release of the luminal cargo

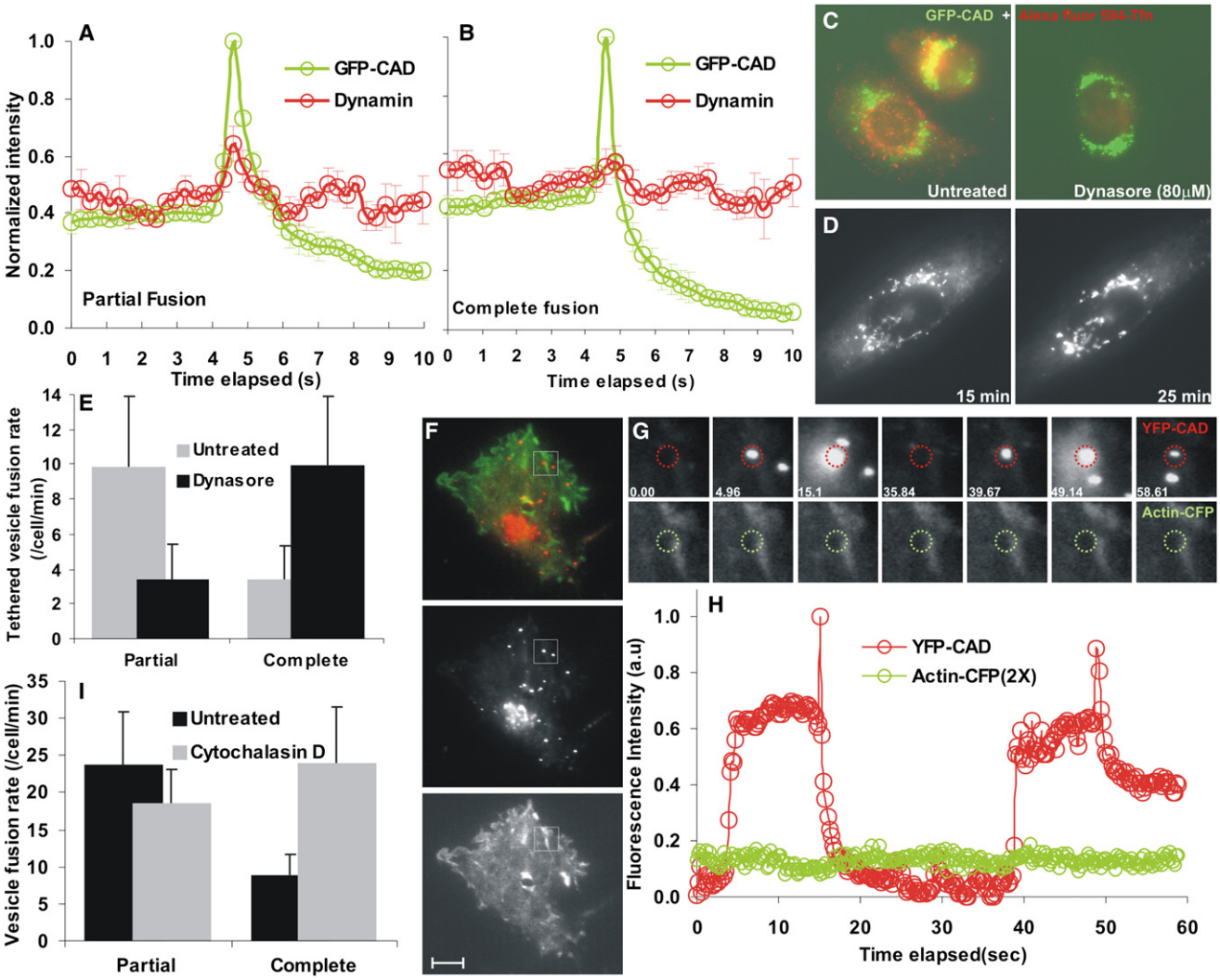

Figure 6. Role of Dynamin and Actin in Post-Golgi Vesicle Exocytosis

(A and B) Luminal cargo GFP-CAD and dynamin2(aa)-mCherry were simultaneously imaged by TIRFM in AP21988-treated cells. Averaged intensity traces for GFP and mCherry for 29 vesicles undergoing kiss-and-run fusion (A) and 27 vesicles undergoing complete fusion (B). Traces were aligned to the point of secretion (peak of GFP-CAD fluorescence), and the error bars represent the SEM.

(C) GFP-CAD expressing cells treated or not treated for 10 min with dynasore were labeled with transferrin (Tfn), and extracellular Tfn was acid washed prior to fixing. Only untreated cells (left) show Tfn-containing vesicles (red).

(D) Cells treated for 20 min with 80 μM dynasore were treated with AP21988 to allow exit of the luminal cargo from the ER, and the cargo was monitored continuously; two of the time points after ligand addition shown here demonstrate that this cargo fails to traffic out of the Golgi.

(E) Rate of exocytosis of 121 GFP-CAD-labeled vesicles (from seven cells) that were tethered to the cell surface at the start of imaging was monitored after treatment of cells with AP21988 alone (untreated) or an additional 10 min treatment with 80 μM dynasore.

(F) A cell expressing the luminal cargo YFP-CAD and actin-CFP was imaged by TIRFM after treatment with AP21988. The scale bar represents 10 μm.

(G) The boxed region in (F) is magnified. The lower panel shows actin, and the upper panel shows YFP-CAD images, at the time points indicated.

(H) Quantification of YFP and CFP fluorescence from the region in (G) marked by dotted circle.

(I) Rate of exocytosis in nine cells treated with AP21988 alone (untreated) and with 2 μM cytochalasin D as judged by luminal cargo.

The error bars in (E) and (I) represent the standard deviation.

from the ER, cells were immunostained for endogenous dynamin. Dynamin was only occasionally present on the post-Golgi vesicles at the cell surface (Figure S3B). To test whether dynamin associates with vesicles at the time of fusion, we expressed dynamin2(aa)-mCherry and monitored its distribution in live cells. The signal/noise for dynamin was weaker than that for dynamin at endocytic vesicles, so we averaged signals from multiple events. A rapid (<1 s) burst of dynamin occurred at the site of fusion of vesicles that released their cargo partially (Figure 6A, 27 events), and no detectable increase in dynamin occurred for vesicles that released their cargo completely (Figure 6B, 29 events). To test for a functional consequence on exocytosis,

we blocked dynamin activity. Dynamin activity is required for budding of biosynthetic cargo carrying vesicles from the TGN (Cao et al., 2000; Kreitzer et al., 2000). This prevented the use of agents that chronically block dynamin activity (dynamin siRNA, dominant-negative dynamin mutants, or function-blocking antibodies) to test the role of dynamin in regulating the fusion step for post-Golgi vesicles. This requires transient and rapid block of dynamin activity, for which we used dynasore—a cell-permeant small-molecule inhibitor of dynamin's GTPase activity (Macia et al., 2006). Consistent with previously reported effects of a chronic block in dynamin function, treatment of cells expressing luminal cargo with 80 μM dynasore for 10 min fully blocked endocytosis of transferrin (Figure 6C) and prevented release of cargo from the Golgi (Figure 6D). At the concentrations and duration we used, dynasore had no detectable effect on cell viability, based on trypan blue dye exclusion (S.M.S., unpublished data). Moreover, the effect of dynasore was reversible: after dynasore washout, luminal cargo-containing post-Golgi vesicles reappeared at the cell surface and fused in a manner that was indistinguishable from their behavior prior to dynasore treatment (Movie S4). To assess the role of dynamin in regulating the post-Golgi vesicle fusion pore, we allowed the luminal cargo to be packaged into post-Golgi vesicles for 20 min, and then 10 min after adding dynasore we analyzed the fate of cell membrane-tethered vesicles. Cells treated with dynasore had a 3-fold increase in the number of fusions that resulted in complete release of cargo (9.9 ± 4 versus 3.4 ± 1.9; $p = 0.001$) and a similar decrease in the number of partial release events (3.4 ± 2 versus 9.8 ± 4.1; $p = 0.0005$) (Figure 6E), indicating that the GTPase activity of dynamin regulates kiss-and-run fusion of post-Golgi vesicles.

F-actin mediates dynamin and clathrin-dependent vesicle fission and has been implicated in postfusion retrieval of *Xenopus* egg granules (Sokac and Bement, 2006). To investigate whether actin assembly contributes to premature closure of the post-Golgi vesicle fusion pore, we transiently expressed actin-CFP in cells expressing the YFP-tagged luminal cargo (Figure 6F). We observed no change in F-actin at the site of fusion irrespective of the nature of release—complete or partial (Figures 6G and 6H). Thus, within our detection limits, F-actin buildup at the site of fusion is not required for pinching off and closure of fusion pore during partial fusion. To test whether F-actin affects the kiss-and-run fusion of post-Golgi vesicles, we treated cells simultaneously with AP21988 and 2 μM cytochalasin D for 30 min and then imaged exocytosis of luminal cargo. Cytochalasin D treatment resulted in over 2-fold increase in the number of fusions that completely released their cargo (24.0 ± 7.5 versus 8.9 ± 2.9; $p = 10^{-5}$), while the rate of partial fusion remained unchanged (18.5 ± 4.5 versus 23.8 ± 7.1; $p = 0.2$). This caused a small increase in the total rate of fusions (42.6 ± 9.7 versus 32.7 ± 8.0; $p = 0.03$).

DISCUSSION

Imaging the secretion of membrane and luminal cargo simultaneously from individual post-Golgi vesicles has yielded several unexpected observations of the regulation of the secretion of post-Golgi cargo.

(1) We obtained unambiguous evidence for kiss-and-run exocytosis of post-Golgi vesicles and found that it is the dominant mode of biosynthetic cargo secretion. The fusing vesicles had various fates, including incomplete release of luminal and membrane contents, incomplete release of luminal and no release of membrane contents, and complete release of the luminal and membrane contents.

(2) Kiss-and-run fusion has previously been observed in Ca^{2+}-regulated exocytosis and the molecules implicated in determining this fusion fate regulate the Ca^{2+}-sensitivity of fusion. However, the exocytosis of post-Golgi vesicles is insensitive to both influx of extracellular Ca^{2+} and efflux of Ca^{2+} from the vesicle lumen (Figure 4). These results suggest that either the post-Golgi vesicle exocytic SNAREs are not sensitive to Ca^{2+} increase or that accessory factors make them Ca^{2+} insensitive. Regardless of the mechanism, our results indicate that Ca^{2+} does not regulate formation or expansion of the fusion pore during all forms of exocytosis and that kiss-and-run fusion of post-Golgi vesicles is not regulated by calcium.

(3) Interference with the synthesis or activity of clathrin, dynamin, and actin, proteins that regulate curvature and fission of vesicle membrane during endocytosis, affects the nature of post-Golgi vesicle fusion (Figures 5 and 6). Based on the following observations, we conclude that the effects of these proteins on fusion are not through their role in clathrin mediated endocytosis: First, clathrin builds up gradually at the endocytic spot (Merrifield et al., 2002; Rappoport and Simon, 2003), which is not observed at the sites of kiss-and-run fusions. All of the clathrin on these vesicles is present before the vesicle appears at the cell surface (Figures 5B and 5C, Movie S3). Second, there is no burst of actin around the time of vesicle pinching (Figures 6E–6G), as has been shown for endocytic vesicles (Merrifield et al., 2002). Third, after the detachment from the cell membrane, endocytic vesicles rapidly move out of the evanescent field (Merrifield et al., 2005). In contrast, post-Golgi cargo-containing vesicles remained at the cell surface, often fusing again, sometimes multiple times, until their cargo was released (Figures 3D and 3E).

Thus, the modulation of fusion fate of post-Golgi vesicles appears to be a result of premature termination of cargo release due to a direct role of clathrin, dynamin, and actin in regulating the exocytic machinery rather than a competition between exo- and endocytosis. Direct regulation of exocytic cargo release by clathrin and dynamin could involve binding and sequestering SNAREs, resulting in inefficient fusion (Antonny, 2004). Such a role has been demonstrated for the dynamin homolog (Vps1p) in yeast (Peters et al., 2004). However, regulation by only binding and sequestering SNAREs cannot explain the observed change in the nature of fusions caused by a rapid block in the dynamin GTPase activity (Figure 6E). A mechanochemical mode of action of dynamin in regulating fusion pore has been suggested for DCVs, according to which kiss-and-run fusion of DCVs is regulated by dynamin but not clathrin (Tsuboi et al.,

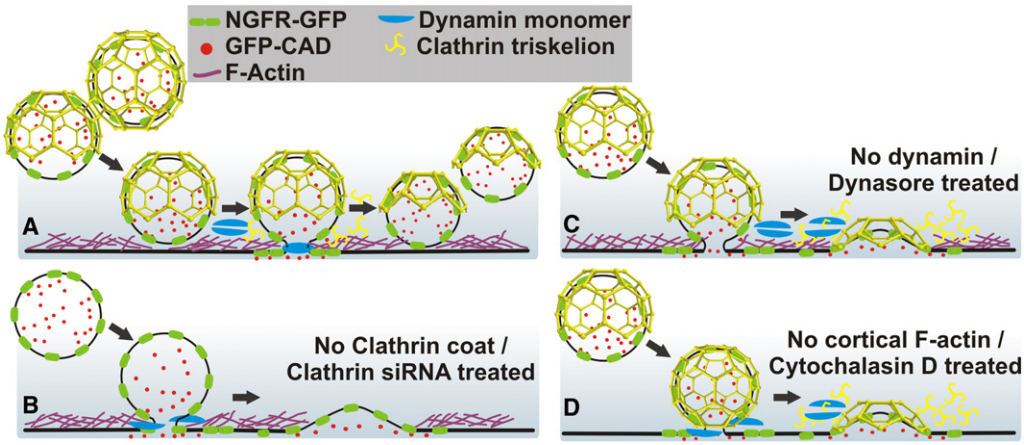

Figure 7. Model for Regulation of the Final Steps of Post-Golgi Vesicle Exocytosis

Presence of clathrin on the vesicle, actin on the cell membrane and dynamin on the neck of the fusing vesicle restricts fusion pore expansion and severing the neck of the vesicle causing partial fusion (A). Lack of clathrin (B), functional dynamin (C), or cortical F-actin (D) relieves the restriction on the fusion pore expansion, causing an increase in complete fusion. Lack of clathrin and cortical F-actin also minimizes physical barrier to the fusion machinery resulting in increased number of total fusions.

2004). However, our results demonstrate that clathrin and dynamin both play a role in restricting the expansion of the post-Golgi vesicle fusion pore. Similarly, clathrin may have a mechanical or mechanochemical role to play in maintaining vesicle curvature, inhibiting flattening, or recruiting molecules that cause scission. Clathrin found on a partially releasing vesicle is present before the vesicle arrives at the cell membrane (Figures 5B and 5C). Thus, as has been shown for TGN derived vesicles (Puertollano et al., 2003) post-Golgi vesicles may obtain their clathrin at the TGN.

Disruption of F-actin also increases the rate of complete and total release. This suggests that disruption of clathrin or actin allows those vesicles to fully fuse that are normally unable to fuse or fuse partially. As no assembly of F-actin is detected at the time of fusion, the mechanism by which F-actin disassembly increases complete fusion is plausibly through the effect on disassembly of cortical F-actin. Disassembly of cortical actin could reduce steric hindrance on vesicle fusion and flattening or allow components of the fusion machinery to diffuse more readily in the plasma membrane and better assemble, causing increased complete fusions. This is consistent with our previous observations that disrupting actin shortens the time between when a vesicle arrives at the plasma membrane and releases its cargo (Schmoranzer and Simon, 2003).

Our observations are consistent with a model for regulation of post-Golgi vesicle fusion pore expansion involving clathrin, actin, and dynamin (Figure 7). According to this model, clathrin and dynamin prevent complete release by restricting the expansion of the fusion pore, severing the neck of the fusion pore, or both (Figure 7A). We suggest that restrictions imposed on partially fusing vesicles slow down vesicle flattening such that the fusion pore neck stays open for longer periods. This is consistent with the observation that luminal cargo is released faster from vesicles undergoing complete fusion compared to those undergoing kiss-and-run fusion (Figure 3F). Additionally, clathrin on the vesicle and cortical F-actin act as barriers, restricting the ability of a fusion pore to form; thus, their absence should increase the total number of fusion events, which is what was observed (Figures 5F, 6E, and 6I). A longer life of the neck of the fusion pore allows a short burst of dynamin assembly that further restricts the expansion of the fusion pore and/or causes its scission resulting in partial fusion (Figures 6A and 7A). However, in vesicles where dynamin does not assemble at the neck or when the dynamin activity is blocked, the release of cargo goes to completion (Figures 6B, 6E, and 7C).

These results raise the question of whether there is a physiological relevance of kiss-and-run fusion of post-Golgi vesicles. One possible role may be to allow rapid retrieval of the Golgi-resident proteins that traffic to the cell surface. Another related role could be in allowing the cell membrane to locally regulate the extent of membrane and luminal cargo secreted by a post-Golgi vesicle. As such, these results are important for understanding the control over secretion of post-Golgi cargo. Additionally, in view of the ongoing controversy regarding whether kiss-and-run fusion does (Gandhi and Stevens, 2003; Aravanis et al., 2003) or does not (Dickman et al., 2005; Ryan et al., 1996) exist, our work provides a system where the regulation of this process can be studied. The interplay we demonstrate between the basal exocytic and endocytic machineries suggests that these processes may have evolved as one instead of two distinct processes for controlling intracellular membrane traffic.

EXPERIMENTAL PROCEDURES

Cell Culture and Treatments

Human fibrosarcoma cells HT1080 were cultured in DMEM supplemented with 10% FBS (Invitrogen, Carlsbad, CA) in 5% CO_2 at 37°C. For imaging, cells were plated onto glass coverslips (Fisher Scientific, Pittsburgh, PA) or on glass bottom dishes (MatTek, Ashland, MA) and imaged in OptiMEM (Invitrogen). Cells were transfected with effectene (QIAGEN, Valencia, CA) or Lipofectamine 2000 (Invitrogen). Transiently transfected cells were imaged within 72 hr of transfection. To release the cargo from ER, an aqueous solution of AP21988 (1 mM, ARIAD Gene Therapeutics, MA) was diluted in OptiMEM

and added to the cells at the final concentration of 2 μM for the desired period prior to imaging. Stocks for FM4-64, BAPTA-AM (Invitrogen) and ionomycin (Sigma Aldrich, St. Louis, MO) were prepared in DMSO and diluted appropriately in OptiMEM for use. For immunodetection, we used goat anti-dynamin II polyclonal antibody (SantaCruz Biotechnology, Santa Cruz, CA), mouse anti-CLC monoclonal antibody clone CON.1 (Covance Research Products, Denver, PA), and mouse anti-CHC monoclonal antibody clone 23 (BD Biosciences Pharmingen, San Diego, CA). For clathrin knockdown, siRNA (AACCUGCG GUCUGGAGUCAAC) described for CHC knockdown in human cells (Hinrichsen et al., 2003) and the siGLO Red transfection control siRNA were obtained from Dharmacon (Chicago, IL). Cells were cotransfected with both these RNAs using Oligofectamine (Invitrogen), and 72 to 96 hr after transfection siGLO labeling was used to identify siRNA transfected cells.

Microscopy and Data Analysis

Through-the-objective TIRFM and epifluorescence microscopy were performed with an inverted Olympus IX-70 microscope with an APO 60× 1.45 NA TIR objective (Olympus Scientific, Melville, NY) equipped with a 12-bit cooled CCD camera (ORCA-ER, Hamamatsu Photonics, Hamamatsu, Japan). The depth of the evanescent field was kept between 100 and 150 nm. The camera, the Mutech MV1500 image acquisition card (Billerica, MA), and the mechanical shutters (Uniblitz, Vincent Associates, Rochester, NY) were controlled by MetaMorph (Molecular Devices, Downingtown, PA). The microscope was enclosed in a home-built chamber for temperature control, and all imaging was performed at 37°C. For TIRFM, fluorophores were excited with 442 nm He-Cd, a 543 nm He-Ne laser, and a tunable Argon laser (Melles Griot, Carlsbad, CA). For epifluorescence, a Xenon short arc lamp (Ushio Inc., Japan) was used. Emission filters used include 480/40, 515/30 or 525/50, 550/50, and 580 lp. Dual-color TIRFM was carried out by simultaneous excitation of both fluorophores, and their emission was spectrally separated with an emission splitter (Dual-View, Optical Insights, Santa Fe, NM) equipped with the band pass filters mentioned above. All filters, dichroics, and polychroics were from Chroma Technologies (Brattleboro, VT). Data analysis was performed with MetaMorph software (Molecular Devices). Statistical significance was measured with the Students' t test, and the significance is reported as p values.

SUPPLEMENTAL DATA

Supplemental Data include three figures and four movies and can be found with this article online at http://www.cell.com/supplemental/S0092-8674(09)00581-9.

ACKNOWLEDGMENTS

We thank Thomas Kirschhausen for providing us with dynasore and DsRed-CLC, Jennifer Lippincott-Schwartz for $VSVG_{ts}$, and Claire Atkinson for Dynamin2(aa)-mCherry. We thank lab members and others who offered helpful suggestions during the course of this work and Patrick Bhola for comments on the manuscript. Knut Wittkowski helped us with some of the statistical analysis, and the work was funded by grants from the National Science Foundation (BES-0620813) and the National Institutes of Health (P20 GM072015 to S.M.S. and R01AR055686 to J.K.J.). J.K.J. designed the research, performed the experiments, analyzed data, and wrote the paper, all with help from S.M.S. V.M.R. contributed new reagents.

Received: April 29, 2008
Revised: February 9, 2009
Accepted: April 17, 2009
Published: June 25, 2009

REFERENCES

Ales, E., Tabares, L., Poyato, J.M., Valero, V., Lindau, M., and Alvarez de Toledo, G. (1999). High calcium concentrations shift the mode of exocytosis to the kiss-and-run mechanism. Nat. Cell Biol. *1*, 40–44.

Antonny, B. (2004). SNARE filtering by dynamin. Cell *119*, 581–582.

Aravanis, A.M., Pyle, J.L., and Tsien, R.W. (2003). Single synaptic vesicles fusing transiently and successively without loss of identity. Nature *423*, 643–647.

Archer, D.A., Graham, M.E., and Burgoyne, R.D. (2002). Complexin regulates the closure of the fusion pore during regulated vesicle exocytosis. J. Biol. Chem. *277*, 18249–18252.

Barclay, J.W., Aldea, M., Craig, T.J., Morgan, A., and Burgoyne, R.D. (2004). Regulation of the fusion pore conductance during exocytosis by cyclin-dependent kinase 5. J. Biol. Chem. *279*, 41495–41503.

Barclay, J.W., Morgan, A., and Burgoyne, R.D. (2005). Calcium-dependent regulation of exocytosis. Cell Calcium *38*, 343–353.

Beckers, C.J.M., and Balch, W.E. (1989). Calcium and GTP: essential components in vesicular trafficking between the endoplasmic reticulum and Golgi apparatus. J. Cell Biol. *108*, 1245–1256.

Cao, H., Thompson, H.M., Krueger, E.W., and McNiven, M.A. (2000). Disruption of Golgi structure and function in mammalian cells expressing a mutant dynamin. J. Cell Sci. *113*, 1993–2002.

Chen, J.L., Ahluwalia, J.P., and Stamnes, M. (2002). Selective effects of calcium chelators on anterograde and retrograde protein transport in the cell. J. Biol. Chem. *277*, 35682–35687.

Dickman, D.K., Horne, J.A., Meinertzhagen, I.A., and Schwarz, T.L. (2005). A slowed classical pathway rather than kiss-and-run mediates endocytosis at synapses lacking synaptojanin and endophilin. Cell *123*, 521–533.

Edwardson, J.M., and Daniels-Holgate, P.U. (1992). Reconstitution in vitro of a membrane-fusion event involved in constitutive exocytosis. A role for cytosolic proteins and a GTP-binding protein, but not for Ca2+. Biochem. J. *285*, 383–385.

Elhamdani, A., Azizi, F., and Artalejo, C.R. (2006). Double patch clamp reveals that transient fusion (kiss-and-run) is a major mechanism of secretion in calf adrenal chromaffin cells: high calcium shifts the mechanism from kiss-and-run to complete fusion. J. Neurosci. *26*, 3030–3036.

Gandhi, S.P., and Stevens, C.F. (2003). Three modes of synaptic vesicular recycling revealed by single-vesicle imaging. Nature *423*, 607–613.

Gong, L.W., Di Paolo, G., Diaz, E., Cestra, G., Diaz, M.E., Lindau, M., De Camilli, P., and Toomre, D. (2005). Phosphatidylinositol phosphate kinase type I gamma regulates dynamics of large dense-core vesicle fusion. Proc. Natl. Acad. Sci. USA *102*, 5204–5209.

Graham, M.E., O'Callaghan, D.W., McMahon, H.T., and Burgoyne, R.D. (2002). Dynamin-dependent and dynamin-independent processes contribute to the regulation of single vesicle release kinetics and quantal size. Proc. Natl. Acad. Sci. USA *99*, 7124–7129.

Harata, N.C., Aravanis, A.M., and Tsien, R.W. (2006). Kiss-and-run and full-collapse fusion as modes of exo-endocytosis in neurosecretion. J. Neurochem. *97*, 1546–1570.

Hinrichsen, L., Harborth, J., Andrees, L., Weber, K., and Ungewickell, E.J. (2003). Effect of clathrin heavy chain- and alpha-adaptin-specific small inhibitory RNAs on endocytic accessory proteins and receptor trafficking in HeLa cells. J. Biol. Chem. *278*, 45160–45170.

Holroyd, C., Kistner, U., Annaert, W., and Jahn, R. (1999). Fusion of endosomes involved in synaptic vesicle recycling. Mol. Biol. Cell *10*, 3035–3044.

Holroyd, P., Lang, T., Wenzel, D., De Camilli, P., and Jahn, R. (2002). Imaging direct, dynamin-dependent recapture of fusing secretory granules on plasma membrane lawns from PC12 cells. Proc. Natl. Acad. Sci. USA *99*, 16806–16811.

Jaiswal, J.K., and Simon, S.M. (2007). Imaging single events at the cell membrane. Nat. Chem. Biol. *3*, 92–98.

Jaiswal, J.K., Andrews, N.W., and Simon, S.M. (2002). Membrane proximal lysosomes are the major vesicles responsible for calcium-dependent exocytosis in nonsecretory cells. J. Cell Biol. *159*, 625–635.

Jaiswal, J.K., Chakrabarti, S., Andrews, N.W., and Simon, S.M. (2004). Synaptotagmin VII restricts fusion pore expansion during lysosomal exocytosis. PLoS Biol. *2*, 1224–1232.

Jaiswal, J.K., Fix, M., Takano, T., Nedergaard, M., and Simon, S.M. (2007). Resolving vesicle fusion from lysis to monitor calcium-triggered lysosomal exocytosis in astrocytes. Proc. Natl. Acad. Sci. USA *104*, 14151–14156.

Katz, B. (1971). Quantal mechanism of neural transmitter release. Science *173*, 123–126.

Kreitzer, G., Marmorstein, A., Okamoto, P., Vallee, R., and Rodriguez-Boulan, E. (2000). Kinesin and dynamin are required for post-Golgi transport of a plasma-membrane protein. Nat. Cell Biol. *2*, 125–127.

Kreitzer, G., Schmoranzer, J., Low, S.H., Li, X., Gan, Y., Weimbs, T., Simon, S.M., and Rodriguez-Boulan, E. (2003). Three-dimensional analysis of post-Golgi carrier exocytosis in epithelial cells. Nat. Cell Biol. *5*, 126–136.

Lew, D.J., and Simon, S.M. (1991). Characterization of constitutive exocytosis in the yeast Saccharomyces cerevisiae. J. Membr. Biol. *123*, 261–268.

Macia, E., Ehrlich, M., Massol, R., Boucrot, E., Brunner, C., and Kirchhausen, T. (2006). Dynasore, a cell-permeable inhibitor of dynamin. Dev. Cell *10*, 839–850.

Mayorga, L.S., Beron, W., Sarrouf, M.N., Colombo, M.I., Creutz, C., and Stahl, P.D. (1994). Calcium-dependent fusion among endosomes. J. Biol. Chem. *269*, 30927–30934.

Merrifield, C.J., Feldman, M.E., Wan, L., and Almers, W. (2002). Imaging actin and dynamin recruitment during invagination of single clathrin-coated pits. Nat. Cell Biol. *4*, 691–698.

Merrifield, C.J., Perrais, D., and Zenisek, D. (2005). Coupling between clathrin-coated-pit invagination, cortactin recruitment, and membrane scission observed in live cells. Cell *121*, 593–606.

Miller, S.G., and Moore, H.P. (1991). Reconstitution of constitutive secretion using semi-intact cells: regulation by GTP but not calcium. J. Cell Biol. *112*, 39–54.

Newton, A.J., Kirchhausen, T., and Murthy, V.N. (2006). Inhibition of dynamin completely blocks compensatory synaptic vesicle endocytosis. Proc. Natl. Acad. Sci. USA *103*, 17955–17960.

Palade, G. (1975). Intracellular aspects of the process of protein synthesis. Science *189*, 867.

Patterson, G.H., Hirschberg, K., Polishchuk, R.S., Gerlich, D., Phair, R.D., and Lippincott-Schwartz, J. (2008). Transport through the Golgi apparatus by rapid partitioning within a two-phase membrane system. Cell *133*, 1055–1067.

Peters, C., and Mayer, A. (1998). Ca2+/calmodulin signals the completion of docking and triggers a late step of vacuole fusion. Nature *396*, 575–580.

Peters, C., Baars, T.L., Buhler, S., and Mayer, A. (2004). Mutual control of membrane fission and fusion proteins. Cell *119*, 667–678.

Porat, A., and Elazar, Z. (2000). Regulation of intra-Golgi membrane transport by calcium. J. Biol. Chem. *275*, 29233–29237.

Puertollano, R., van der Wel, N.N., Greene, L.E., Eisenberg, E., Peters, P.J., and Bonifacino, J.S. (2003). Morphology and dynamics of clathrin/GGA1-coated carriers budding from the trans-Golgi network. Mol. Biol. Cell *14*, 1545–1557.

Rappoport, J.Z., and Simon, S.M. (2003). Real-time analysis of clathrin-mediated endocytosis during cell migration. J. Cell Sci. *116*, 847–855.

Rivera, V.M., Wang, X., Wardwell, S., Courage, N.L., Volchuk, A., Keenan, T., Holt, D.A., Gilman, M., Orci, L., Cerasoli, F., Jr., et al. (2000). Regulation of protein secretion through controlled aggregation in the endoplasmic reticulum. Science *287*, 826–830.

Rollins, C.T., Rivera, V.M., Woolfson, D.N., Keenan, T., Hatada, M., Adams, S.E., Andrade, L.J., Yaeger, D., van Schravendijk, M.R., Holt, D.A., et al. (2000). A ligand-reversible dimerization system for controlling protein-protein interactions. Proc. Natl. Acad. Sci. USA *97*, 7096–7101.

Ryan, T.A., Smith, S.J., and Reuter, H. (1996). The timing of synaptic vesicle endocytosis. Proc. Natl. Acad. Sci. USA *93*, 5567–5571.

Schmoranzer, J., and Simon, S.M. (2003). Role of microtubules in fusion of post-Golgi vesicles to the plasma membrane. Mol. Biol. Cell *14*, 1558–1569.

Schmoranzer, J., Goulian, M., Axelrod, D., and Simon, S.M. (2000). Imaging constitutive exocytosis with total internal reflection fluorescence microscopy. J. Cell Biol. *149*, 23–32.

Sokac, A.M., and Bement, W.M. (2006). Kiss-and-coat and compartment mixing: coupling exocytosis to signal generation and local actin assembly. Mol. Biol. Cell *17*, 1495–1502.

Stevens, C.F., and Williams, J.H. (2000). "Kiss and run" exocytosis at hippocampal synapses. Proc. Natl. Acad. Sci. USA *97*, 12828–12833.

Tsuboi, T., McMahon, H.T., and Rutter, G.A. (2004). Mechanisms of dense core vesicle recapture following "kiss and run" ("cavicapture") exocytosis in insulin-secreting cells. J. Biol. Chem. *279*, 47115–47124.

Wang, C.T., Grishanin, R., Earles, C.A., Chang, P.Y., Martin, T.F., Chapman, E.R., and Jackson, M.B. (2001). Synaptotagmin modulation of fusion pore kinetics in regulated exocytosis of dense-core vesicles. Science *294*, 1111–1115.

Wang, C.T., Bai, J., Chang, P.Y., Chapman, E.R., and Jackson, M.B. (2006). Synaptotagmin-Ca2+ triggers two sequential steps in regulated exocytosis in rat PC12 cells: fusion pore opening and fusion pore dilation. J. Physiol. *570*, 295–307.

Williams, D.A., Fogarty, K.E., Tsien, R.Y., and Fay, F.S. (1985). Calcium gradients in single smooth muscle cells revealed by the digital imaging microscope using Fura-2. Nature *318*, 558–561.

Zhang, Z., and Jackson, M.B. (2008). Temperature Dependence of Fusion Kinetics and Fusion Pores in Ca2+-triggered Exocytosis from PC12 Cells. J. Gen. Physiol. *131*, 117–124.